

Development of 1D+4DVAR data assimilation of radar reflectivity in JNoVA

Yasutaka Ikuta¹ and Yuki Honda

Numerical Prediction Division, Japan Meteorological Agency

Japan Meteorological Agency (JMA) has been operating meso-scale model (MSM), and a four-dimensional variational (4DVAR) data assimilation system based on JMA non-hydrostatic model (JNoVA; Honda et al. 2005) to provide the initial condition of MSM. We have been developing a new approach of ‘1D+4DVAR’ technique of data assimilation system using a radar reflectivity to improve analysis of water vapor and precipitation forecast. In the new approach, a one-dimensional (1D) pseudo observation data of relative humidity (RH) are retrieved by radar reflectivity, and retrieved RH data are assimilated as conventional data in JNoVA. Caumont et al. (2010) reported that the precipitation forecast is improved by using the combination of such 1D retrieval and a three-dimensional variational (3DVAR) data assimilation method (1D+3DVAR) in AROME.

The 1D retrieval method of the pseudo observation of RH employs a best estimate based on Bayes’ theorem (Caumont et al. 2010). In the best estimate, the radar simulator (Ikuta and Honda 2010) plays an important role as an observation operator. The conditional expectation of RH is defined by:

$$E(x) = \int x \cdot p(y = y_o | x = x_{true}) p(x = x_{true}) dx$$
$$= \sum_i x_i W_i(y_o) / \sum_j W_j(y_o) \quad \text{with} \quad W_i \equiv \exp \left\{ -\frac{1}{2} (y_o - y_{s,i})^T R_{z,\beta}^{-1} (y_o - y_{s,i}) - J_p \right\},$$

where x_i is model state of RH, y_o is reflectivity observation, y_s is simulated reflectivity and W_i is weight. In particular, we have added penalty term J_p which is function of height innovation to the weight in this study. The x_i and W_i are given by supported database which is made from the radar simulator outputs (Fig. 1). The 1D+4DVAR data assimilation has an advantage of avoiding the difficulties such as estimating individual type of the hydrometeors from the radar reflectivity because of strongly nonlinear relation between reflectivity and these hydrometeors.

The analysis-forecast cycle experiment demonstrated an improvement of hydrometeors representation as an initial condition. Figure 2 shows that the representation of the simulated and observed reflectivity of Fukuoka radar site. The distribution of radar reflectivity simulated by the first guess is different from that of observed reflectivity, indicating that the first guess has displacement error of simulated hydrometeors distribution. This displacement error is successfully corrected after 1D+4DVAR data assimilation. A forecast experiment is conducted to compare the 33 hours MSM forecast with different analysis methods for the period from 20 July to 26 July 2009. As a result, the equitable threat score (Fig. 3a) and bias score (Fig. 3b) of 1D+4DVAR experiment (referred to as ‘‘Test’’) show an improvement of precipitation forecast than 4DVAR experiment without radar reflectivity assimilation (referred to as ‘‘Control’’) in the early hours of the forecast. Especially, the sudden drop of bias score around FT=3 in the Control experiment is improved in the Test experiment, suggesting that the 1D+4DVAR data assimilation improves analysis of water vapor field (Fig. 4).

References

- Honda, Y., M. Nishijima, K. Koizumi, Y. Ohta, K. Tamiya, T. Kawabata and T. Tsuyuki, 2005: A pre-operational variational data assimilation system for a non-hydrostatic model at the Japan Meteorological Agency: Formulation and preliminary results. *Quart. J. Roy. Meteor. Soc.*, **131**, 3465-3475.
- Caumont, O., V. Ducrocq, É. Wattrelot, G. Jaubert, S. Pradier-vabre, 2010: 1D+3DVar assimilation of radar reflectivity data: a proof of concept. *Tellus A, Volume 62*, 173–187.
- Ikuta, Y. and Y. Honda, 2010: Fuzzy Verification of Hydrometeors in a High-resolution Model Using a Radar Simulator. *CAS/JSC WGENE Res. Activ. Oceanic Modell.*, **40**, 05.09 – 05.10
- Yuter, S. E., and R. A. Houze Jr., 1995: Three-dimensional kinematic and microphysical evolution of Florida cumulo-nimbus. Part II: Frequency distributions of vertical velocity, reflectivity, and differential reflectivity. *Mon. Wea. Rev.*, **123**, 1941–1963.

¹ ikuta@met.kishou.go.jp

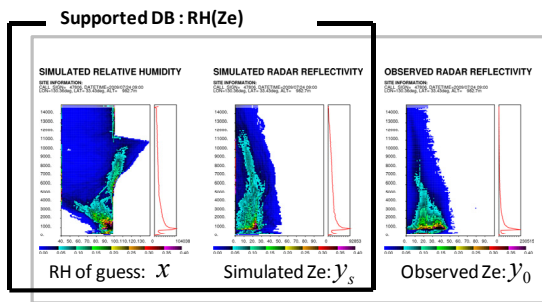


Fig. 1 CFADs (contour frequency by altitude diagram, Yuter and Houze 1995) of simulated RH, reflectivity and observed reflectivity. Supported database is composed by simulated RH and reflectivity.

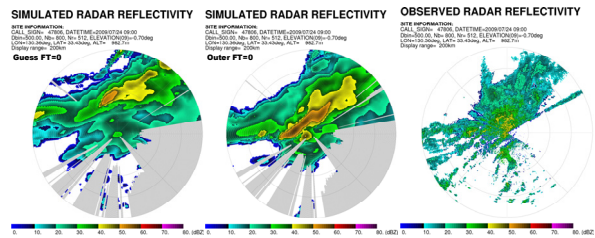


Fig. 2 PPI (plan position indicator) of elevation 0.7° . Simulated reflectivity by guess (left), simulated reflectivity by initial condition of MSM (middle), and observed reflectivity (right). The gray color region represent beam blockage by topography.

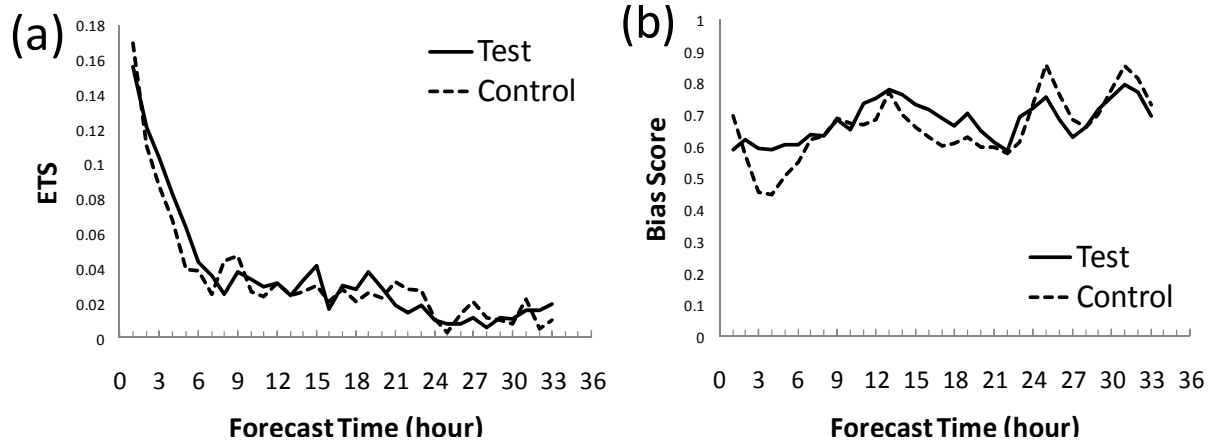


Fig. 3 Comparison of Test experiment and Control experiment of precipitation verification against RA. Time series of (a) equitable threat score (ETS) and (b) Bias Score. Solid line is the scores of Test, and dashed line is that of Control. Moreover, verification region is Japan, verification grid size is 20km and threshold is 10mmh^{-1} .

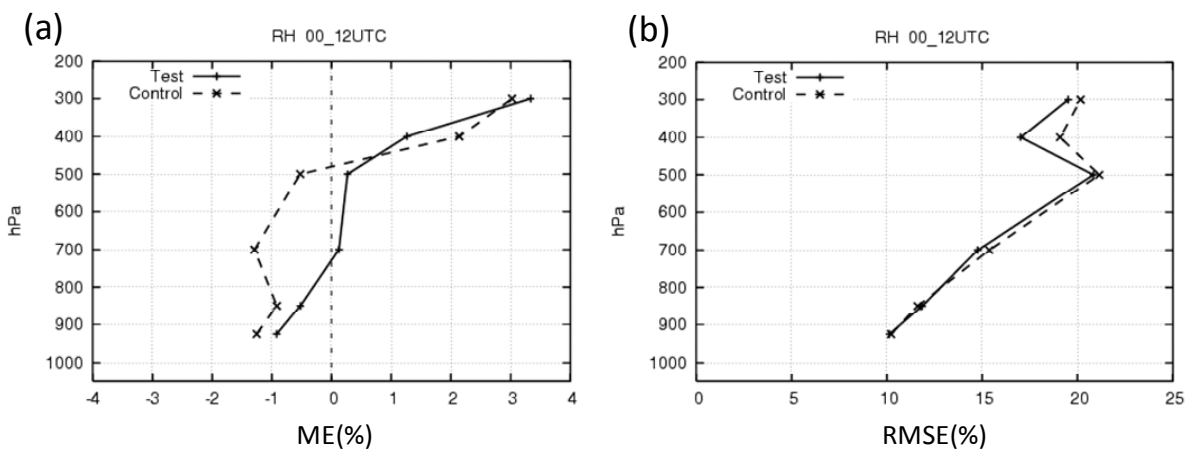


Fig. 4 Comparison of Test experiment and Control experiment of RH profile verification against sonde observation. (a) Mean error (ME) and (b) Root mean square error (RMSE). Solid line is the scores of Test, and dashed line is that of Control. Moreover, verification region is Japan and forecast time is 3 hours.